Study of 2800-nm OH/H_2O feature at Compton-Belkovich Thorium Anomaly (CBTA) in the far side of the Moon using Chandrayaan-1 Moon Mineralogy Mapper (M^3) data. Satadru Bhattacharya, Prakash Chauhan and Ajai, Space Applications Centre (ISRO), Ahmedabad – 380 015, India (satadru@sac.isro.gov.in).

Introduction: One of the major objectives of Chandrayaan-1 Moon Mineralogy Mapper (M^3) was to detect 2.8- and 3-µm absorption features arising due to the presence of OH- and/or H_2O-bearing silicates [1] on the otherwise anhydrous surface of the Moon. On the Moon, the OH/H_2O complex absorption feature near 3 µm was found to be widely distributed having strongest absorptions at cooler high latitudes and at several fresh feldspathic craters [1]. The same observation had also been confirmed by the Deep Impact spacecraft extended mission (EPOXI) [2] and by the Visible and IR Mapping Spectrometer (VIMS) onborad Cassini [3]. Also, very high circular polarization ratio has been observed in the Chandrayaan-1 Mini-SAR data [4] in the north polar regions of the Moon that could be attributed to the presence of water-ice in the premanently shadowed craters at the north pole and the same was later confirmed by the impact of Lunar Crater Observation and Sensing Satellite (LCROSS) spacecraft into a permanently shadowed crater on the south pole region of the Moon where it reported evidence of water along with other materials in the ejecta [5]. Here, we report the detection of very strong OH- and/or H_2O feature from the central part of Compton-Belkovich Thorium Anomaly (CBTA) region (61.1ºN, 99.5ºE) in the farside of the Moon. Chandrayaan-1 M3 Level 2 thermally corrected reflectance data from optical period "OP2C" have been used for the present study.

Study Area: The central part, i.e., the study area, is characterized by high reflectance and Digital Terrain Model indicates positive relief features that could be of volcanic origin [6]. Presence of irregular depressions within the topographic high was observed by [6] that could represent collapse features associated with volcanism. LRO Diviner thermal measurements indicate that the region is enriched in silica or alkali feldspar whereas the Lunar Prospector Gamma-Ray Spectrometer (LPGRS) measurements show high thorium contents associated with the high reflectance central part of CBTA. These observations collectively hint towards the unique occurrence of non-mare silicic volcanism in the far side of the Moon [6].

Methods: False Color Composite (FCC) of the study area is shown in Fig. 1 where, Red channel has been assigned to 930-nm M^3 band, Green to 2018-nm M^3 band and Blue to the 2816-nm M^3 channel. The CBTA region appears bright yellow in such a FCC (Fig. 1). An area of 3×3 pixels (red box in Fig. 1) is chosen for generating the mean spectra from the study area as shown in Fig. 2A. The spectra does not show any 1000- and/or 2000-nm mafic feature and overall albedo of the surface is ~26% (bright). However, a strong doublet feature, centered at ~2896 nm, has been observed in the M^3 spectra throughout the central part of the CBTA region, which could be attributed to the O-H stretch fundamentals near 2800 and 2900 nm typical of materials containing hydroxyl groups (OH) (Fig. 2A). The strength of the 2800-nm doublet feature varies from ~4-15% in the studied area.

In the present study, we have characterized the 2800-nm spectral region in order to search for evidence of water in the CBTA region. We have obtained a new Integrated Band Depth (IBD) for the 2800-nm feature as given below:

$$\sum_{n=0}^{9} 1 - \frac{R(2617+40n)}{Rc(2617+40n)}$$

Details of the terms used in the above equation can be found in [7]. FCC has been generated by assigning Red channel to IBD-2800-nm, Green to IBD-1000-nm [7] and Blue to IBD-2000-nm [7]. In such a band combination, OH/H_2O-bearing lunar regoliths will appear in red to pink, whereas pyroxenes-bearing lithologies will appear in cyan color.

Observations and Discussion: Spectra from the central part of CBTA are mostly dominated by a strong doublet feature near 2800 nm. The shorter and longer wavelength band minima of the doublet occurs at ~2816 and 2936 nm respectively. Apart from the doublet, a relatively broad, weaker feature centered at 2936-nm has also been observed locally. As already discussed, the strength of the OH/H_2O absorption feature varies from ~4-14% within the central region. Figures 3A, 3B and 3C represent IBD-1000-nm, IBD-2000-nm and IBD-2800-nm respectively, and Fig. 3D shows FCC of the study area generated using IBD-2800-nm as red, IBD-1000-nm as Green and IBD-2000-nm as Blue. It is evident from Figs. 3a and 3b that the area lacks any strong mafic feature. However, weak to moderate 2000-nm feature has been observed locally within the region. In IBD-2800-nm image, the central part of CBTA appears as bright region in an otherwise dark surrounding (Fig. 3c). In the IBD-based FCC of the studied area, the central part of CBTA appears red due to the presence of strong OH/H_2O feature near 2800 nm (Fig. 3d). At places, we have also observed strong (strength ~10%) OH/H_2O 2800-nm feature in association with a weak spinel feature (strength ~5%) at 2000-

nm that completely lacks a 1000-nm mafic feature (Fig. 2B). The strong OH/H2O feature is only restricted within the high reflectance CBHRF region of [5].

At CBTA, OH and/or H_2O is primarily associated with the positive-relief, high-reflectance (CBHRF) volcanic construct that might have formed due to the eruption of a relatively high-viscosity silicic lava [5].

Conclusions: Based on the present observations as obtained from M3 data, there are several options to consider for the origin of water and hydroxyl molecules in the studied site. Possibilities could be categorized into two classes: endogenic and exogenic. (1) Endogenic: During the late stage silicic magmatism, the residual melt gets enriched in volatiles. Such a volatile enriched late stage hydrothermal fliud from the lunar interior could possibly be the source of hydroxyl and/or water in the study area at a local scale. This is also supported by the highly silicic composition of the volcanic construct at the central part of CBTA as given by [6]. (2) Exogenic: Another probable source of OH and perhaps H_2O could be solar-wind-proton-induced hydroxylation. Studies by [1] clearly showed the compositional effects as seen in M^3 data on the OH/H_2O absorption strength having more absorption for highland materials probably because of the higher abundance of volatiles in the highlands than in the mare [8]. It is evident from the present study that OH/H_2O molecules have greater affinity towards highly silicic regolith materials over the surrounding anorthitic highland soils, if the source is solar-wind-proton-induced hydroxylation. Detailed lab-based and simulation studies need to be carried out in order to understand the processes that has lead to the enrichment of hydroxyl and/or water on/in the CBTA region and also to establish correlation between the concentration of hydroxyl and/or water with that of the highly silicic surface composition in the central part of CBTA.

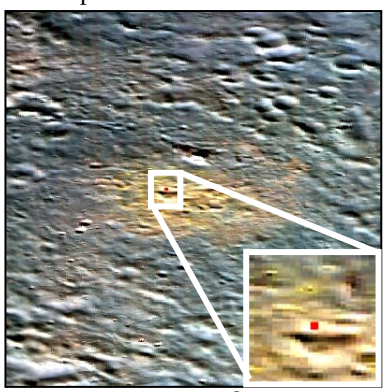

Fig 1. FCC (R: 930-nm M^3 channel; G: 2018-nm M^3 channel; B: 2816-nm M^3 channel) of central part of CBTA. Mean spectra of 3×3 pixels (red box in the FCC) from the central part of the study area is presented in Fig 2A.

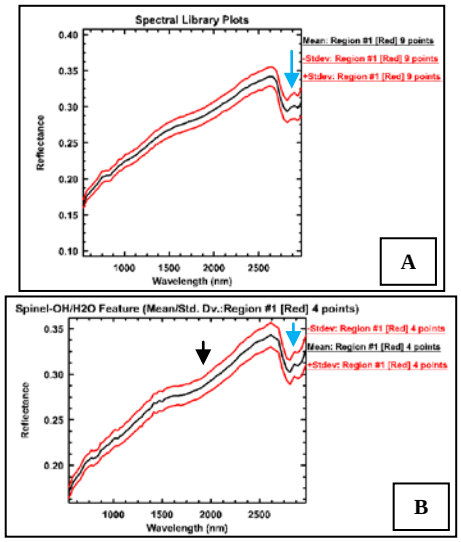

Fig 2. A. Mean spectra from the central part of CBTA showing strong OH/H_2O doubletfeature (blue arrow) near 2800-nm; B. A strong OH/H_2O feature (blue arrow) at ~2800 nm along with a weak spinel feature at 2000-nm (black arrow) from the CBTA region.

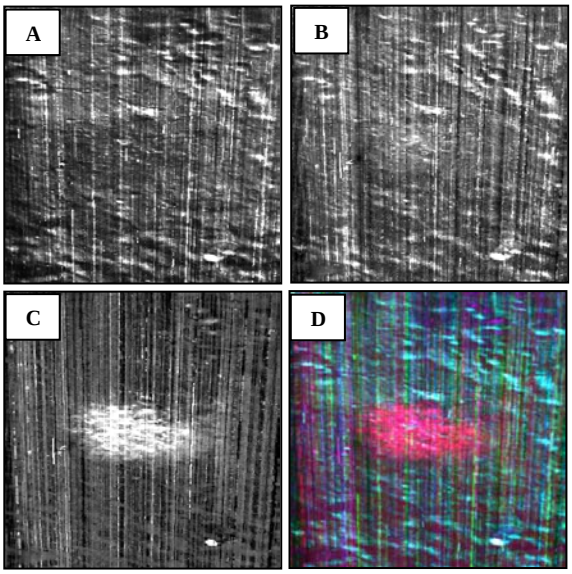

Fig 3. A. 1000-nm IBD; B. 2000-nm IBD; C. 2800-nm IBD; D. IBD-based FCC generated by assigning Red channel to IBD-2800, Green channel to IBD-1000 and Blue channel to IBD-2000. OH/H_2O-bearing lithology of central part of CBTA appears red in the IBD-based FCC.

References: [1] Pieters C. M. et al. (2009) *Science* 326, 568. [2] Sunshine J. M. et al. (2009) *Science 326*, 565. [3] Clark R. N. (2009) *Science* 326, 562. [4] Spudis P. D. et al. (2010) *GRL, L06204*. [5] McCord T. B. et al. (2010) *LPS XXXXI*, Abstract #1860. [6] Jollif B. L. et al. (2011) *LPS XXXXII*, Abstract #2224. [7] Mustard J. F. et al. (2011) *JGR, 116*, E00G12. [8] McCord T. B. et al. (2011) *JGR, 116*, E00G05.